Low-Complexity Doubly Selective Channel Simulation Using Multidimensional Discrete Prolate Spheroidal Sequences

Florian Kaltenberger
ARC Seibersdorf research GmbH
Donau-City-Strasse 1
1220 Vienna, Austria
Email: florian.kaltenberger@arcs.ac.at

Thomas Zemen
Forschungszentrum Telekommunkation Wien
Donau-City-Strasse 1
1220 Vienna, Austria
Email: thomas.zemen@ftw.at

Christoph W. Ueberhuber
Vienna University of Technology
Wiedner Hauptstrasse 8-10/101
1040 Vienna, Austria
Email: c.ueberhuber@tuwien.ac.at

***Abstract*— This paper presents a low-complexity algorithm for the simulation of time-variant frequency-selective geometry based channel models. The algorithm approximately calculates the time-variant transfer function of the channel in the subspace spanned by *multidimensional discrete prolate spheroidal (DPS) sequences*. The only parameters of the subspace are the maximum Doppler shift and the maximum delay of the channel as well as the channel bandwidth and the observed time interval.**

By adjusting the dimension of the subspace, it is possible to trade complexity for accuracy. On a 16 bit fixed-point arithmetic processor, the computational complexity can be reduced by an order of magnitude compared to a conventional sum-of-sinusoids implementation.

I. Introduction

The modeling and simulation of wireless mobile communication channels is very important for the design and test of receiver algorithms. Especially for the test of mobile radio hardware devices, real-time implementations of such channel models are required.

In [1], [2], the time-variant channel is described as a stochastic process and correlated variates of this process are calculated. A different approach is pursued in [3], [4], where the time-variant impulse response is calculated as a superposition of different propagation paths using geometry based ray tracing principles (see Fig. 1). Geometric models are considered to be more realistic and accurate. However, they come with a higher computational complexity, since for every propagation path, every time instance and every delay or frequency bin a complex exponential has to be evaluated.

A special case, which is also known as Clarke's model [5] is obtained by placing the scatterers on a circle around the receiver according to a uniform distribution. This model is often used as a mathematical reference model. The computational complexity of Clarke's model can be reduced by a factor of four by placing the scatterers equidistantly on the circle [6]. However, the second order statistics of Jakes' simplification do not match the ones of Clarke's model. An enhanced version of Jakes' simplification was proposed by Zheng [7] and Zemen applied corrections for low velocities [8].

In [9] a new subspace based algorithm for simulating time-variant frequency-flat geometry based channel models was presented, which allows for a complexity reduction by more than an order of magnitude. It uses discrete prolate spheroidal (DPS) sequences as bases for a subspace representation of the time-variant channel transfer function. The choice of DPS bases is connected with the following observations: (i) the fading process of the channel is bandlimited by the maximum Doppler shift and (ii) the channel simulation is carried out for a finite time interval.

This paper extends the method from [9] to time-variant frequency-selective channels. Therefore we use *two-dimensional* DPS sequences [10] to span a subspace for the time-frequency channel transfer function. The two-dimensional DPS bases are chosen based on the observation, that the fading process of the time-frequency channel transfer function is bandlimited by the essential support of the Doppler-delay spreading function and that the channel simulation is carried out for a finite time interval *and* for a finite frequency band. The computational complexity of the model does not increase significantly by adding another dimension.

The proposed subspace representation of the channel is very well suited for implementation on a real-time hardware channel simulator like the *ARC SmartSim* [11]. By adjusting the dimension of the subspace, the bias of the subspace representation can be made smaller than the numerical precision given by the hardware, allowing to trade accuracy for efficiency.

The paper is organized as follows. The notation is introduced in Section II. Section III explains the signal model of time-variant frequency-selective channels. In Section IV, we derive the subspace representation of the time-variant frequency-selective channel transfer function. Results from numerical experiments are given in Section V and conclusions are drawn in Section VI.

II. Notation

Vectors are denoted by $\boldsymbol{v}$ and matrices by $\mathbf{V}$. Their elements are denoted by $\boldsymbol{v}_i$ and $\mathbf{V}_{i,l}$. The transpose of a vector or a matrix is given by $\cdot^{\mathrm{T}}$ and its conjugate transpose by $\cdot^{\mathrm{H}}$. The norm of vector $\boldsymbol{a}$ is denoted through $\|\boldsymbol{a}\|$. The Kronecker product is denoted by $\otimes$. $|X|$ denotes the number of elements of X if X is a discrete index set or the area of X is X is a continuous region. Multidimensional sequences are denoted by $v_{\boldsymbol{m}}$, where $\boldsymbol{m} \in I$ and I is a multidimensional index set. When the index set is finite and ordered then we may collect the elements of the sequence in a vector $\boldsymbol{v}$.

III. Signal Model

Time-variant frequency selective channels are described by their impulse response $h(t,\tau)$ or equivalently by their time-variant transfer function $L(t,f) = \int h(t,\tau)e^{-2\pi j f \tau}\mathrm{d}\tau$. The latter one is used to develop a subspace representation of the channel. Using a Fourier transform, we can easily switch between those representations.

We model the time-variant frequency-selective channel as superposition of P individual propagation paths (see Fig. 1). The channel's time-variant transfer function can then be written as

$$L'(t,f) = \sum_{p=0}^{P-1} \eta_p e^{2\pi j \omega_p t} e^{-2\pi j \tau_p f}, \tag{1}$$

where η_p is the complex path gain, ω_p is the Doppler shift and τ_p is the delay of path $p = 0,\ldots,P-1$. Further, we assume that the energy of all paths is normalized to one $\mathcal{E}\{\sum_{p=0}^{P-1} |\eta_p|^2\} = 1$.

A. Sampled Signal Model

The channel can only be measured, respectively simulated for a finite channel bandwidth. This corresponds to applying an ideal bandpass filter to the channel. Let $R(f)$ denote the filter in the frequency domain. The filtered transfer function is given by

$$L(t,f) = L'(t,f) \cdot R(f). \tag{2}$$

The sampled transfer function then writes

$$\begin{aligned} g_{m,q} &= L(mT_S, qF_S) \\ &= \sum_{p=0}^{P-1} \eta_p e^{j2\pi\nu_p m} e^{-j2\pi\theta_p q} R(qF_S), \end{aligned} \tag{3}$$

where m is the discrete time with sample rate $1/T_S$, q is discrete frequency with sample rate $1/F_S$, $\nu_p = \omega_p T_S$ is the normalized Doppler frequency, and $\theta_p = \tau_p F_S$ is the normalized delay of path p.

The sample rate F_S must fulfill $F_S \leq 1/\tau_{\max}$ where $\tau_{\max}$ is the maximum delay of the channel. The sample rate T_S must fulfill $T_S \leq 1/(2\omega_{\mathrm{Dmax}})$ where ω_{Dmax} is the maximum Doppler shift of the channel. The latter one is always fulfilled in mobile communication channels whereas F_S has to be chosen according to the scenario.

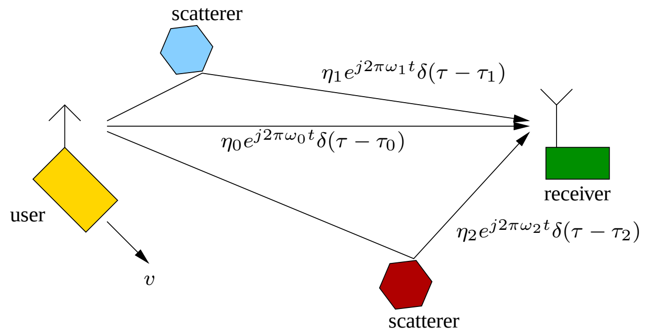

Fig. 1. Time-variant frequency-selective multi-path propagation model for a wireless radio channel. The signals sent from the transmitter, moving at speed v, arrive at the receiver. Each path p has attenuation η_p, time delay τ_p and Doppler shift ω_p

IV. Subspace representation of doubly selective channels

In this section we will develop a subspace representation of the sampled time-varying transfer function $g_{m,q}$ (3). The subspace representation is based on the observations made in Sec. IV-A. In Sec. IV-B, the two-dimensional DPS bases are introduced. Sec. IV-C and IV-D deal with the subspace representation and the approximate subspace projection respectively. Finally in Sec. IV-E, a complexity analysis and the memory requirements of the algorithm are given.

A. Observations

Firstly, the simulation of the channel is only done for a finite length M and a finite number of frequencies Q, i. e. $g_{m,q}$ is only observed in the index set

$$I = \underbrace{\{0,\ldots,M-1\}}_{=:I_0} \times \underbrace{\{-\lfloor Q/2\rfloor,\ldots,\lceil Q/2\rceil - 1\}}_{=:I_1}. \tag{4}$$

The number of frequency bins $Q = B/F_S$ and the number of samples $M = T/T_S$, where B is the observed bandwidth and T is the observed time.

Secondly, the variation of $g_{m,q}$ in time and frequency is limited by the support W of the Doppler-delay spreading function

$$g_{m,q} = \iint_W S(\nu,\theta) e^{2\pi i m\nu} e^{-2\pi i q\theta} \mathrm{d}\nu \mathrm{d}\theta. \tag{5}$$

Furthermore $g_{m,q}$ is highly oversampled in time *and* frequency, i. e. $|W| \ll 1$.

The bandlimit or passband region W is assumed to be

$$W = \underbrace{[-\nu_{\mathrm{Dmax}}, \nu_{\mathrm{Dmax}}]}_{=:W_0} \times \underbrace{[0, \theta_{\max}]}_{=:W_1}, \tag{6}$$

where ν_{Dmax} is the maximum (one-sided) normalized Doppler shift and $\theta_{\max}$ is the maximum normalized delay. This assumption corresponds to modeling the channel as wide sense stationary with uncorrelated scatterers (WSS-US).

B. Two-Dimensional Discrete Prolate Spheroidal Sequences

Multidimensional DPS sequences $v_{\boldsymbol{m}}^{(d)}(W,I),\ \boldsymbol{m}\in\mathbb{Z}^N$ are a generalization of [12] to N dimensions. They span a subspace of $\ell^2(\mathbb{Z}^N)$, that contains all bandlimited N-dimensional sequences with passband region $W\subset\mathbb{R}^N$, whose energy is concentrated in the index set $I\subset\mathbb{Z}^N$. The exact definition and some properties of multidimensional DPS sequences can be found in [13]–[15].

In [10] it is shown, that if the passband region W and the index set I can be written as Cartesian products, the multidimensional sequences can be calculated as a Kronecker product of onedimensional DPS sequences. In particular, for the two-dimensional case, if I and W are defined by (4) and (6), then the DPS vector $\boldsymbol{v}^{(d)}(W,I)$ and its eigenvalue $\lambda_d(W,I)$ can be calculated as

$$\boldsymbol{v}^{(d)}(W,I)=\boldsymbol{v}^{(d_0)}(W_0,I_0)\otimes\boldsymbol{v}^{(d_1)}(W_1,I_1) \tag{7}$$
$$\lambda_d(W,I)=\lambda_{d_0}(W_0,I_0)\lambda_{d_1}(W_1,I_1), \tag{8}$$

where $d_0=\lfloor d/Q\rfloor,\ d_1=d \mod Q$. The DPS vectors are sorted such that their eigenvalues are in descending order

$$\lambda_0(W,I)>\lambda_1(W,I)>\ldots>\lambda_{D-1}(W,I). \tag{9}$$

The one-dimensional DPS sequence in the frequency domain can be calculated according to

$$\begin{aligned}&v^{(d_1)}_{q-\lfloor Q/2\rfloor}([0,\theta_{\max}],\{-\lfloor Q/2\rfloor,\ldots,\lceil Q/2\rceil-1\})=\\&\quad\tilde{v}^{(d_1)}_q([-\frac{\theta_{\max}}{2},\frac{\theta_{\max}}{2}],\{0,\ldots,Q-1\})e^{-\pi j\theta_{\max}q}.\end{aligned} \tag{10}$$

The shifting of the DPS sequences in (10) is done to take into account the non-symmetric interval $\theta\in[0,\theta_{\max}]$ of the time delays [16].

C. Subspace Representation

Based on the observations of the last subsection, we choose the subspace to be the one spanned by the first D two-dimensional DPS sequences $v^{(d)}_{m,q}(W,I)$, where W and I are defined by (6) and (4) respectively.

Denote by $\boldsymbol{g}$ the vector of elements of the time-variant transfer function $g_{m,q}$ indexed lexicographically,

$$\boldsymbol{g}=[g_{0,-\lfloor Q/2\rfloor},g_{0,-\lfloor Q/2\rfloor+1},\ldots,g_{M-1,\lceil Q/2\rceil-1}]^T. \tag{11}$$

Further, collect the DPS vectors $\boldsymbol{v}^{(d)}(W,I),\ d=0,\ldots,D-1$, in the columns of the matrix

$$\mathbf{V}=[\boldsymbol{v}^{(0)}(W,I),\ldots,\boldsymbol{v}^{(D-1)}(W,I)]. \tag{12}$$

Then the subspace projection of the time-variant transfer function can be written as

$$\boldsymbol{\alpha}=\mathbf{V}^H\boldsymbol{g}, \tag{13}$$
$$\hat{\boldsymbol{g}}=\mathbf{V}\boldsymbol{\alpha}. \tag{14}$$

To calculate the basis coefficients $\boldsymbol{\alpha}$, it is convenient to write

$$\boldsymbol{g}=\sum_{p=0}^{P-1}\eta_p\boldsymbol{e}_p, \tag{15}$$

where $\boldsymbol{e}_p=\boldsymbol{e}_p^{(0)}\otimes\boldsymbol{e}_p^{(1)}$ and

$$\boldsymbol{e}_p^{(0)}=[1,e^{2\pi j\nu_p},\ldots,e^{2\pi j\nu_p(M-1)}]^T, \tag{16}$$
$$\boldsymbol{e}_p^{(1)}=[e^{2\pi j\theta_p\lfloor Q/2\rfloor},\ldots,1,\ldots,e^{-2\pi j\theta_p\lceil Q/2\rceil-1}]^T. \tag{17}$$

Then, the basis coefficients $\boldsymbol{\alpha}_d$ can be calculated as

$$\boldsymbol{\alpha}_d=\boldsymbol{v}^{(d)}(W,I)^H\boldsymbol{g}=\sum_{p=0}^{P-1}\eta_p\underbrace{\boldsymbol{v}^{(d)}(W,I)^H\boldsymbol{e}_p}_{=:\gamma_{d,p}}. \tag{18}$$

Omitting the dependence on W and I and using (7),

$$\begin{aligned}\gamma_{d,p}&=(\boldsymbol{v}^{(d_0)}\otimes\boldsymbol{v}^{(d_1)})^H(\boldsymbol{e}_p^{(0)}\otimes\boldsymbol{e}_p^{(1)})\\&=\boldsymbol{v}^{(d_0)H}\boldsymbol{e}_p^{(0)}\otimes\boldsymbol{v}^{(d_1)H}\boldsymbol{e}_p^{(1)}\\&=\gamma_{d_0,p}\cdot\gamma_{d_1,p},\end{aligned} \tag{19}$$

where $\gamma_{d_0,p}$ and $\gamma_{d_1,p}$ are the basis coefficients obtained by projecting $\boldsymbol{e}_p^{(0)}$ and $\boldsymbol{e}_p^{(1)}$ on the subspace spanned by the corresponding one-dimensional DPS vectors respectively.

D. Approximate Subspace Projection

To calculate $\gamma_{d_0,p}$ and $\gamma_{d_1,p}$ approximately but efficiently in $\mathcal{O}(1)$ operations, we take advantage of the *DPS wave functions* $U_{d_j}(f)$ which are defined as the amplitude spectrum of a onedimensional DPS sequence $v_m^{(d_j)},\ j=0,1$ [12].

$$U_{d_j}(f)=\epsilon_{d_j}\sum_{m=0}^{M-1}v_m^{(d_j)}e^{-j\pi(M-1-2m)f}, \tag{20}$$

where $\epsilon_d=1$, if d even, and $\epsilon_d=j$ if d odd.

Using (19) and (10) it can be shown that

$$\gamma_{d_0,p}=\frac{1}{\epsilon_{d_0}}e^{j\pi(M-1)\nu_p}U_{d_0}(\nu_p;\nu_{\mathrm{Dmax}},M) \tag{21a}$$
$$\gamma_{d_1,p}=\frac{1}{\epsilon_{d_1}}e^{\pi j(Q-1)\theta_{\max}/2}U_{d_1}(\theta_{\max}/2-\theta_p;\theta_{\max}/2,Q), \tag{21b}$$

where $\epsilon_d=1$, if d even, $\epsilon_d=i$, if d odd.

In [9] it was shown that $U_{d_j}(f),\ j=0,1$ can be approximately calculated by a simple scaling and shifting of the corresponding DPS sequence. Thus the basis coefficients $\gamma_{d_j,p},\ j=0,1$ can be calculated approximately in $\mathcal{O}(1)$ operations.

Denote by $\tilde{\boldsymbol{\alpha}}_d$ the approximated basis coefficients and by $\tilde{\boldsymbol{g}}=\mathbf{V}\tilde{\boldsymbol{\alpha}}$ the approximate basis representation of the time-variant transfer function.

E. Complexity Analysis and Memory Requirements

The complexity of the subspace representation is calculated in terms of evaluations of complex exponentials (CE), complex multiplications (CM) and complex dotproducts of length P (CDOT(P)).

The approximate basis coefficients $\tilde{\boldsymbol{\alpha}}$ can be calculated in

$$C_{\tilde{\boldsymbol{\alpha}}}=PD(3\,\mathrm{CE}+5\,\mathrm{CM})+D\,\mathrm{CDOT}(P) \tag{22}$$

operations, where the first term accounts for the calculation of the coefficients $\tilde{\gamma}_{d,p}$ in (21), and the second term for the calculation of $\tilde{\boldsymbol{\alpha}}_d$ in (18).

Parameter	Value
Observation time T	$1/1500$ sec
OSF time O_T	2
Blocklength M	$2560 \cdot O_T$
Sample rate $1/T_{\mathrm{S}} = M/T$	$3.84 \cdot O_T$ MHz
Bandwidth B	5 MHz
OSF frequency O_F	$\{10, 100\}$
No. subcarriers Q	$256 \cdot O_F$
Subcarrier spacing $F_S = B/Q$	$76.8 \cdot O_F^{-1}$ kHz
No. paths P	$\{40, 80, 120\}$
Carrier frequency f_c	2 GHz
Mobile velocity $v_{\max}$	100 kmph
Maximum Doppler shift $\omega_{\mathrm{D}\max}$	185 Hz
Maximum Delay spread $\tau_{\max}$	$\{0.4, 3.7\}\mu$s

TABLE I

SIMULATION PARAMETERS FOR THE NUMERICAL EXPERIMENTS.

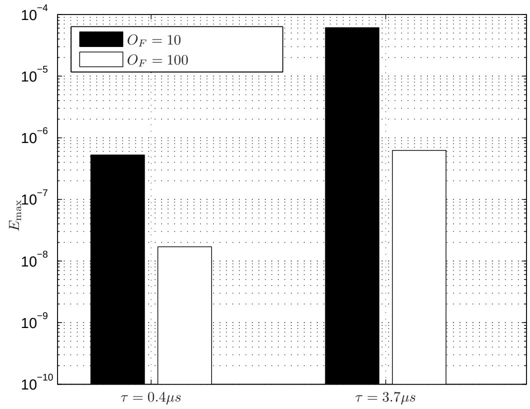

Fig. 2. Approximation error $e^{(D)}$ of the subspace projection for different maximum delays $\tau_{\max}$ and different oversampling factors O_F over the subspace dimension D.

In total, for the evaluation of the approximate subspace representation of the channel (14),

$$C_{\text{DPSS}} = D\text{CDOT}(P) + C_{\tilde{\alpha}}$$

operations are required. On the other hand, the sum-of-sinusoids algorithm (3) needs

$$C_{\text{SoS}} = MQP\,\text{CE} + MQ\,\text{CDOT}(P)$$

operations for every block of length M. It can be seen, that as the number of paths P increases, the complexity of the SoS model increases with slope MQ, whereas the complexity of the subspace model increases with slope D only.

Since the two-dimensional DPS sequences in $\mathbf{V}$ can be calculated as a Kronecker product of one-dimensional sequences (7), only the one-dimensional sequences need to be stored. Therefore, only $MD_0 + QD_1$ elements need to be stored, where D_0 and D_1 are the maximum number of one-dimensional DPS vectors needed to construct the two-dimensional vectors up to the dimension D.

V. NUMERICAL EXPERIMENTS

For the numerical experiments we used the parameters given in Table I. First, the error introduced through the approximations (21) is evaluated. In Sec. V-B, the squared bias of the subspace representation is evaluated. Finally, in Sec. V-C run-time measurements of a Matlab implementation of the channel model are given.

A. Approximation Error

The approximation error is the error that is introduced by using the approximate DPS wave functions [9] to calculate the subspace projection. It is calculated according to

$$e^{(D)} = \mathcal{E}\left\{\frac{1}{MQ}\|\hat{\boldsymbol{g}}^{(D)} - \tilde{\boldsymbol{g}}^{(D)}\|^2\right\}, \tag{23}$$

where the index $\cdot^{(D)}$ denotes the number of basis functions used for the subspace representation. The maximum approximation error $E_{\max} = \max_D\{e^{(D)}\}$ is plotted in Fig. 2 using the parameters from Table I for different oversampling factors (OSFs) in frequency O_F and different maximum delays $\tau_{\max}$ of the channel.

It can be seen, that for channels with a maximum delay of $\tau_{\max} = 3.7 \cdot 10^{-6}$sec a higher OSF in frequency is required to achieve the same approximation error than for channels with a maximum delay of $\tau_{\max} = 0.4 \cdot 10^{-6}$sec. This observation also holds for the approximation in the time domain, where a higher maximum Doppler shift requires a higher OSF in time. In general it can be said, that a higher time-bandwidth product requires higher OSF for the approximation. In any case, the OSF can be chosen such that the approximation error stays below the numerical precision of a 16 bit fixed-point processor. Such a processor has a numerical precision of $2^{-15} \approx 3 \cdot 10^{-5}$.

B. Bias

The squared bias of the subspace representations $\tilde{\boldsymbol{g}}^{(D)}$,

$$\text{bias}_{\tilde{g}}^{(D)} = \mathcal{E}\left\{\frac{1}{MQ}\|\boldsymbol{g} - \tilde{\boldsymbol{g}}^{(D)}\|^2\right\}. \tag{24}$$

is plotted in Fig. 3 for different maximum delays $\tau_{\max}$ and different oversampling factors O_F. It can be seen that: (i) The bias decreases with the subspace dimension and the decrease is steeper for channels with a smaller delay spread $\tau_{\max}$. (ii) After a certain dimension, the bias levels out.

The first observation is explained using again the time-bandwidth product of the DPS sequences. A lower time-bandwidth product implies a lower subspace dimension and a stepper descent of the eigenvalues. The latter is explained by the approximation error identified in the last subsection. A higher OSF O_F induces a better approximation, which induces a lower error floor.

Comparing the results to the numerical precision of a 16 bit fixed-point processor, it can be seen, that for a channel with a delay spread of $\tau_{\max} = 0.4 \cdot 10^{-6}$sec, a subspace dimension of $D = 20$ and an OSF of $O_F = 10$ is needed to achieve the necessary accuracy. On the other hand, for a channel with a delay spread of $\tau_{\max} = 3.7 \cdot 10^{-6}$sec a subspace dimension of $D = 70$ and an OSF of $O_F = 100$ is needed. Note, that the oversampling is only needed for the calculation of the basis coefficients, not for the subspace representation.

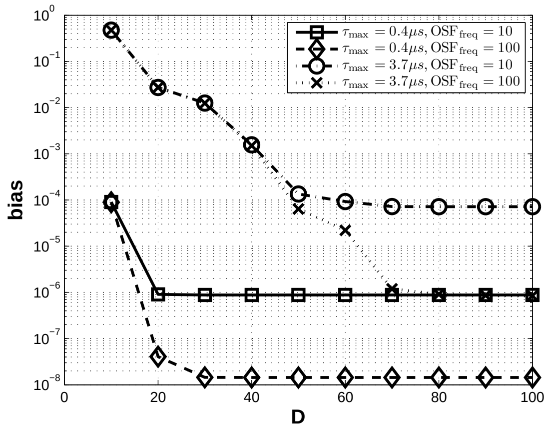

Fig. 3. Bias of the subspace representation $\tilde{\boldsymbol{g}}$ for different maximum delays $\tau_{\max}$ and different oversampling factors O_F over the subspace dimension D.

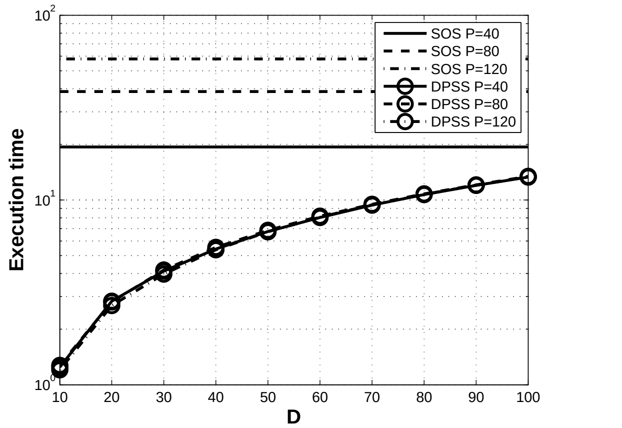

Fig. 4. Runtime of the DPS subspace based channel model (DPSS) and the sum-of-sinusoids (SoS) model over the subspace dimension D

C. Run-time Evaluations

For the run-time evaluations, the approximate subspace representation as well as the original sum-of-sinusoids (SoS) algorithm were implemented in Matlab. Their run-times were compared on a 2.5 GHz Intel Pentium 4 machine with 1 Gbyte RAM. They are plotted for different number of paths in Fig. 4. They match the theoretical evaluations very well.

When comparing the subspace method for a subspace dimension of $D = 20$ with the SoS algorithm with $P = 80$ paths, it can be seen that one order of magnitude can be saved. For a subspace dimension of $D = 70$, still a factor of 5 can be saved, when comparing to the SoS algorithm with $P = 120$ paths.

VI. CONCLUSIONS

We have presented a low-complexity approximate implementation of time-variant frequency-selective channel models that is tailored for implementation on a real-time hardware channel simulator. It uses a representation of the time-variant transfer function in the subspace spanned by the multidimensional DPS sequences. By adjusting the dimension of the subspace, the bias of the subspace representation can be made smaller than the numerical precision given by by the hardware. The subspace projection can be calculated approximately in $\mathcal{O}(1)$ operations. Thus, the complexity can be reduced by an order of magnitude when compared to a conventional sum-of-sinusoids implementation.

Opposed to the simplified channel models of Jakes and Zheng, no assumptions about the placement of the scatterers is assumed. Only the maximum Doppler shift and the maximum delay spread of the channel need to be know. Thus, the method can be used with any geometry based channel model.

ACKNOWLEDGEMENTS

This work was funded by the Wiener Wissenschafts-, Forschungs- und Technologiefonds (WWTF) in the ftw. project Future Mobile Communication Systems (Math+MIMO).

REFERENCES

[1] K. Baddour and N. Beaulieu, "Autoregressive modeling for fading channel simulation," *IEEE Trans. Wireless Commun.*, vol. 4, no. 4, pp. 1650–1662, July 2005.

[2] M. Jachan and G. Matz, "Nonstationarity vector AR modeling of wireless channels," in *Proc. 6th IEEE Workshop on Signal Processing Advances in Wireless Communications (SPAWC)*, New York, USA, June 2005, pp. 648–652.

[3] L. M. Correia, Ed., *Wireless Flexible Personalised Communications*. Wiley, 2001.

[4] H. Hofstetter and G. Steinböck, "A geometry based stochastic channel model for MIMO systems," in *Proceedings of the ITG Workshop on Smart Antennas*, Munich, Germany, January 2004.

[5] R. Clarke, "A statisctical theory of mobile-radio reception," *The Bell Systems Technical Journal*, pp. 957–1000, Jul.–Aug. 1968.

[6] W. Jakes, *Microwave Mobile Communications*. Wiley, 1974.

[7] Y. R. Zheng and C. Xiao, "Simulation models with correct statistical properties for Rayleigh fading channels," *IEEE Trans. Commun.*, vol. 51, no. 6, pp. 920–928, June 2003.

[8] T. Zemen and C. F. Mecklenbräuker, "Time-variant channel estimation using discrete prolate spheroidal sequences," *IEEE Trans. Signal Processing*, vol. 53, no. 9, pp. 3597–3607, September 2005.

[9] F. Kaltenberger, T. Zemen, and C. W. Ueberhuber, "Low complexity simulation of wireless channels using discrete prolate spheroidal sequences," in *Proc. MATHMOD Conference*, Vienna, Austria, February 2006.

[10] ——, "Multidimensional discrete prolate spheroidal sequences," in preparation, 2006.

[11] F. Kaltenberger, G. Steinböck, R. Kloibhofer, R. Lieger, and G. Humer, "A multi-band development platform for rapid prototyping of MIMO systems," in *Proc. ITG Workshop on Smart Antennas*, Duisburg, Germany, April 2005.

[12] D. Slepian, "Prolate spheroidal wave functions, Fourier analysis, and uncertainty - V: The discrete case," *The Bell System Technical Journal*, vol. 57, no. 5, pp. 1371–1430, May-June 1978.

[13] ——, "Prolate spheroidal wave functions, Fourier analysis, and uncertainty - IV: Extensions to many dimensions; generalized prolate spheroidal functions," *The Bell System Technical Journal*, vol. 43, no. 6, pp. 3009–3058, November 1964.

[14] S. Dharanipragada and K. S. Arun, "Bandlimited extrapolation using time-bandwidth dimension," *IEEE Trans. Signal Processing*, vol. 45, no. 12, pp. 2951–2966, December 1997.

[15] D. V. D. Ville, W. Phillips, and I. Lemahieu, "On the n-dimensional extension of the discrete prolate spheroidal window," *IEEE Signal Processing Lett.*, vol. 9, no. 3, pp. 89–91, March 2002.

[16] T. Zemen, H. Hofstetter, and G. Steinböck, "Successive slepian subspace projection in time and frequency for time-variant channel estimation," in *Proceedings of the 14th IST Mobile and Wireless Communication Summit (IST SUMMIT)*, Dresden, Germany, June 19-22 2005.